

Modeling of Corona Streamer Discharge Development ALong an Ice Surface

Boubakeur Zegnini¹, Bachir Alili²

¹ Laboratoire d'études et Développement des Matériaux Semi conducteurs et Diélectriques (LeDMaScD), Amar Telidji University of Laghouat, Algeria, b.zegnini@mail.lagh-univ.dz

² Laboratoire d'études et Développement des Matériaux Semi conducteurs et Diélectriques (LeDMaScD), Amar Telidji University of Laghouat, Algeria,

Abstract

The objective of this paper is to understand the inception of ice surface corona streamers. A validated onset criterion that is useful for practical electrode geometries is presented. The effects of several experimental parameters such as freezing water conductivity and HV electrode radius on the streamer inception parameters of an ice surface have been examined. Empirical models have been proposed, based on elements derived from the inception parameters to account for corona streamer propagation velocity and inception voltage/field on an ice surface. Since the propagation velocity is a power function of the electric field, its value has been expressed in terms of the inception voltage.

1. Introduction

Streamer inception and subsequent propagation is an important precursor of the occurrence of electrical breakdown and flashover in many high voltage configurations in air. Flashover on an ice surface is an extremely complex phenomenon resulting from the interaction between the following factors: electric field, wet and polluted ice surface, presence of air gaps at the ice surface, environmental conditions and the complex geometry of an ice-covered insulator. Therefore, the understanding of the inception and propagation of discharge along those air gaps is important for outdoor insulation design. Several major parameters that strongly influence the phenomena have been considered, including gap configuration, freezing water conductivity and surrounding temperature. Corona inception time, voltage/field inception and streamer propagation velocity are determined using the positive lightning impulse voltage. The results are discussed and used to establish empirical models. These investigations help to support the emergence of new expertise in the field of prevention, more particularly for designing and sizing insulators for regions with a cold climate. The results will also be helpful in establishing mathematical models for predicting flashover on ice-covered insulating surfaces.

2. Physical Model

The physical model used for streamer inception and propagation on the ice surface consists of a rod-plane gap configuration half-submerged in the ice bulk (Figure 1), where the inter-electrode distance d is adjustable. For the purposes of this study, rods with various radii (1.5, 3 and 6 mm), and a fixed interelectrode distance of 35 mm were used.

The electrodes were screwed into a rectangular Plexiglas box, which also served as a mould to form the ice, possible.

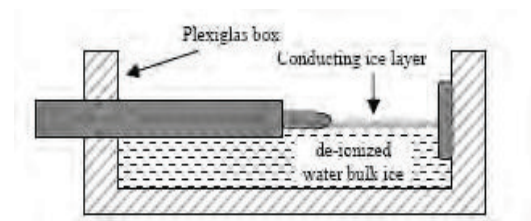


Fig. 1. Vertical section of the physical ice model.

Details of this experimental set-up and the ice mass of the built-up test specimen may be found in previous papers [5, 6]. In this experiment, the discharge is guided along an approximately linear path. A small sharp point at the centre of the lower grounded plane has been found useful [5, 6]. This type of discharge is therefore particularly suited to study the basic processes of corona streamer propagation. In addition to the study of discharge on ice surfaces, corona discharge in the air gaps between the electrodes was also studied, which will be referred to as the air reference case. A standard 1.2/50 μ s positive lightning impulse voltage was applied to the rod to stress the inter-electrode space through an HV impulse generator. The streak sweep duration of the camera used to record the optical phenomena can be varied from 5 ns to 1 ms. The wavelength covered ranges from ultraviolet light to the near infrared region (200 to 850 nm).

3. Modeling parameters

The values of distance used in our tests were selected in the objective to look further into the results obtained in the preceding investigations of the CIGELE [3, 8]. This work had already established the clear influence of the distance inter-electrodes on the process of the discharge. Our values of distance inter-electrodes are $D = 35$ mm and $D = 70$ mm. It should be said as these values were selected according to the limits of the camera observation with sweeping of slit, because the larger the distance is, the more discharge follows a random way and thus tends more to be propagated apart from the zone of observation of the camera. Consequently the selected values of distance seem to us to be a perfect consensus between the importance of this parameter and the performances of the camera.

The radius of curvature of the electrodes being revealed to be a very important parameter in development of the discharge, four values of radius of curvature of the electrode high voltage ($R = 1.5$ mm, 3 mm and 6 mm) were used in our investigations. By carrying out tests with the same distance inter-electrodes (d), these various values of radius of curvature (R) make it possible to analyze another parameter, the d/r .

The various values of conductivity used are $\sigma = 2.5$, 30 and $80 \mu\text{s.cm}^{-1}$. They were selected in agreement with those obtained on the natural sites of white frost. These values having already been useful in the preceding investigations [7, 8], it appears completely natural to again use them in our tests for reasons of comparison and analysis. To obtain water with a certain conductivity, sodium chloride (NaCl) is gradually added in water die-ionized until reaching the desired value. Conductivity obtained is allotted to the layer of ice since it is very difficult to measure with precision the conductivity of the ice.

The values of temperature chosen for our tests were already used in studies former [7,8]. The choice of these same values will make it possible to look further into the results already obtained on the effect of the temperature on the parameters of appearance of the discharge. Our tests were carried out for more the share at the temperature $T = -12^\circ\text{C}$. However two other values, $T = -6^\circ\text{C}$ and $T = -2^\circ\text{C}$, were also used with an aim of looking further into the investigations. These values make it possible to maintain the layer of ice in a dry state. The temperature of the layer of ice is always considered equal to that of the climatic room. The model is always placed sufficiently a long time in the room before the beginning of the tests so that the layer of ice can adopt the room temperature.

4. Modeling of the electric field

The inception electric field, E_{inc} , is obtained by using numerical field calculations computed by Comsol Multiphysics 3.5, integrated engineering software, the 3D electric field calculation model. Geometric plotted graphs of electric field distributions corresponding to 1 V applied to the HV rod, in the presence of an ice layer and in the air reference case are illustrated in Figure 2 and 3. These calculations require the dielectric and conductive parameters of ice such as permittivity and conductivity shown in Table 1.

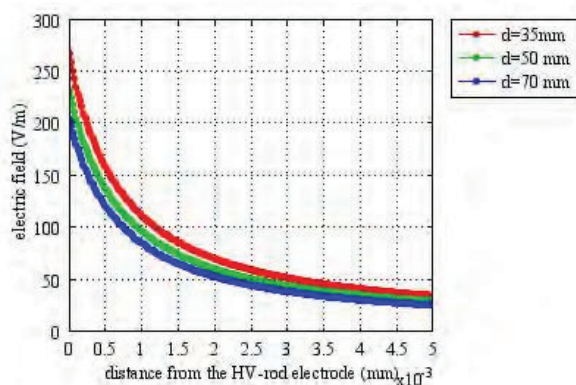


Fig. 2. Electric field distribution for a 35-mm gap distance and 1.5 mm electrode radius for air.

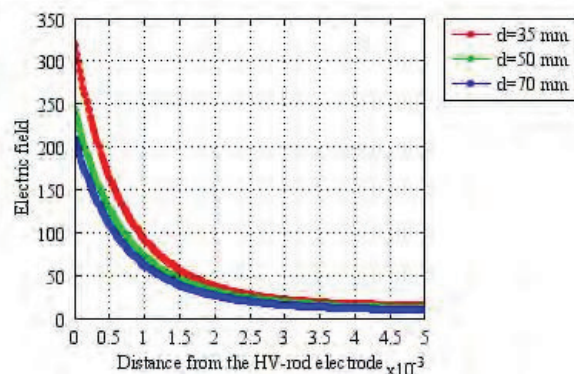


Fig. 3. Electric field distribution for a 35-mm gap distance and 1.5 mm electrode radius without the presence of an ice surface.

In calculating the electric field distribution and maximum field strength, parameters such as form factor and geometry, are generally used. The form factor, F , of a non-uniform field electrode configuration is defined as:

$$F = \frac{E_{\text{mean}}}{E_{\text{max}}} \quad (1)$$

Where E_{mean} is the average field strength of the arrangement, which is the applied voltage over the electrode spacing, usually referred to as gap length, and where E_{max} is the highest field strength between the electrodes. The calculated results of the maximum electric field E_{max} , using Comsol Multiphysics and the form factors of the different gap geometries are listed in Table 1. Values for air are given in brackets.

Table 1: Maximum field and form factors for 35, 50 and 70-mm gap distances.

r (mm)		1,5	3	6
d=35(mm)	E(max) (V/m)	318.801 (266.68)	210.443 (148.56)	151.183 (129.666)
	F	0.0896 (0.1071)	0.1358 (0.1923)	0.1890 (0.2203)
d=50(mm)	E(max) (V/m)	243.028 (231.41)	176.786 (129.63)	135.402 (106.565)
	F	0.0823 (0.0864)	0.1131 (0.1543)	0.1477 (0.1877)
d=70(mm)	E(max) (V/m)	209.870 (203.91)	137.405 (113.71)	117.054 (103.030)
	F	0.0681 (0.0701)	0.1040 (0.1256)	0.1220 (0.1387)

The field threshold of appearance is obtained by numerical simulations carried out using the software Comsol Multiphysics 3.5 allows to characterize and optimize the process of load and to control the applied voltage.

The threshold voltage is the breaking value where ionization appears and thus, a density of space load. In lower part of this limit, the electric field satisfies the equation of Laplace:

$$\nabla^2 V = 0 \quad (2)$$

The application of a tension higher than the tension V_s threshold generates the appearance of a current which involves a disturbance of the distribution of this electric field. By supposing that the mobility of the ions is constant and by taking account only of the zone of drift, the equations governing the electric field in space inter-electrodes are given by the following system:

$$\vec{\nabla} \cdot \vec{E} = \frac{\rho}{\epsilon_0} \quad (3)$$

$$\vec{E} = -\vec{\nabla} V \quad (4)$$

$$\vec{\nabla} \cdot \vec{j} = 0 \quad (5)$$

$$\vec{j} = \rho \cdot \mu \cdot \vec{E} - D_e \cdot \vec{\nabla} \rho \quad (6)$$

With \vec{E} electric field, V electric potential,

$\epsilon_0 = 8.854187817 \cdot 10^{-12} \text{ F/m}$ permittivity of the vacuum, ρ density of load ionic, \vec{j} surface density of current, μ electric mobility of the ions, D_e ionic coefficient of diffusion. The Poisson's equation (3) described the ionized electric field; The equation (4) connect the electric field to the electric potential; the equation (5) express the conservation of the current; the equation (6) connect the density of current ionic to the electric field.

Moreover, speeds of the ions due to the diffusion are in general negligible in front of those resulting from the electric field. Thus what amounts writing that the density of current is proportional to the electric field:

$$\vec{j} = \mu \cdot \rho \cdot \vec{E} \quad (7)$$

The chronological sequence of computations performed during the discharge simulation is shown in figure 2 and 3.

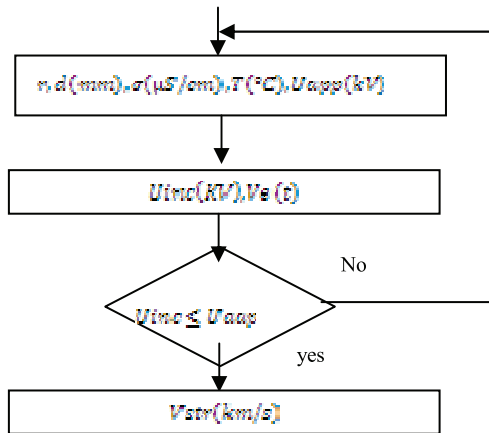


Fig. 4. A general flow chart of the model.

A Script COMSOL program was carried out to calculate the streamer propagation velocity according to the form of the applied impulse voltage. The code starts with some input data. The applied voltage is increased up to the situation in which the potential at the tip of the rod U_{app} is exposed to the ice/air interface, with an overcritical field region $E > E_{inc}$ ahead, within which ionization avalanches can develop and streamers may start to propagate. We assume that the conducting channel is initiated by the inception of the first corona with the initial length fixed to 10^{-6} m [9]. In this case, we applied positive lightning impulse voltage (from 0 ms to 100 ms) duration half-width.

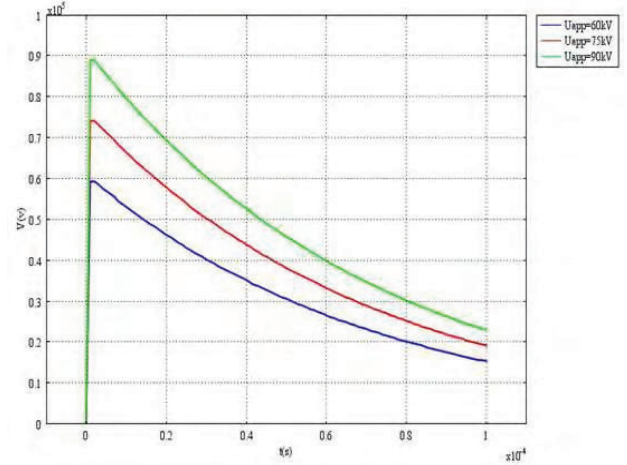


Fig. 5. Waves form of applied positive lightning impulse voltage.

5. Streamer propagation velocity

An important feature essential to the understanding of the interaction between a discharge and a dielectric surface is the velocity of the streamer when it propagates along the surface. This property was investigated by using highly sensitive framing camera. By an appropriate selection of the exposure time, the number of frames and the inter electrode distance, the mean velocity of the streamer can be evaluated for the different investigated surfaces. Figures 6, 7 and 8, show the results of streamer velocity model as a function of the HV electrode radius r to the rod electrode. It can be observed that the streamer velocity augments with an increase in the applied field. Obtained values are more intense in the presence of an ice surface. It was also observed that the higher the freezing water conductivity, the greater the streamer velocity is.

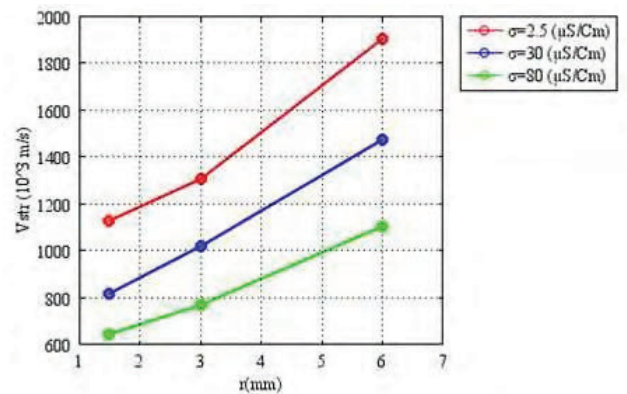


Fig. 6. Streamer propagation velocity as a function of the high voltage electrode radius r at the rod electrode at -2°C

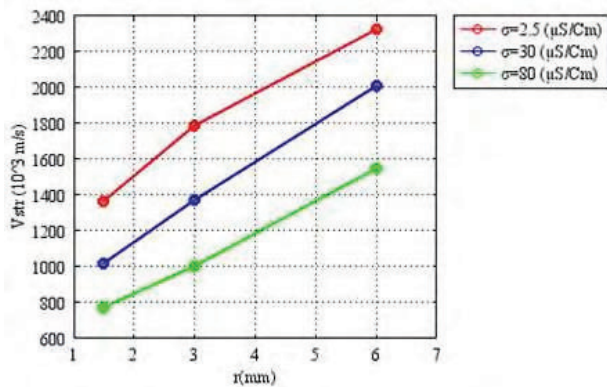


Fig.7. Streamer propagation velocity as a function of the high voltage electrode radius r at the rod electrode at -6°C

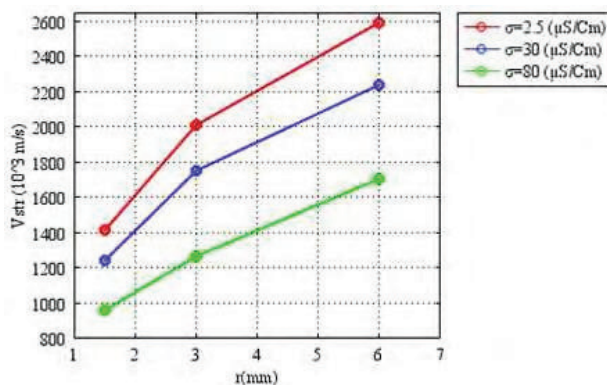


Fig. 8. Streamer propagation velocity as a function of the high voltage electrode radius r at the rod electrode at -12°C

The model presented simulates the development of a corona discharge on an ice surface and in air, essentially on the basis of simplified electrostatic considerations and empirical equations. The simple analytical expressions used give the model good stability and high computation speed. Comparison with experimental data indicated that the model can also take into account some macroscopic parameters influencing the development of discharge on an ice surface, such as freezing water conductivity and surrounding temperature. Further work is necessary to establish more general empirical equations using a wide range of macroscopic parameters. In this connection, the authors will engage in a study to further investigate those points using framing camera and photomultipliers, and they expect to publish their results in a future work.

6. Conclusion

We have just studied in this article the characteristics of the positive streamers in the presence of surface of ice and in the case of the air. Results of simulations carried out on a physical model of configuration stem - plan by using software COMSOL made it possible to note that the presence of the surface of ice influenced considerably the appearance and the development of the streamers. The permittivity of the ice, larger than that of the air is one of the main reasons. Indeed, the strong presence of impurities and the existence of a quasi-liquid layer on surface also seemed being determining factors in the development of the streamers. These two parameters were controlled by the conductivity of the water of congelation and the temperature and

their variation made it possible to show that for a configuration of electrodes given, the field of appearance of the streamers decreases when one increases the conductivity of the water of congelation for the same temperature or when one increases the temperature for a given conductivity.

7. References

- [1] M. Farzaneh and J. Kiernicki, "Flashover problems caused by ice build-up on Insulators", IEEE Trans. on Power Delivery, Vol. 12, No. 4, pp. 1602-1613, 1997.
- [2] M. Farzaneh, "Ice accretion on high voltage conductors and insulators and related phenomena", Phil. Trans. R. Soc. Lond. A, Vol. 358, No. 1776, pp. 2971-3005, 2000.
- [3] M. Farzaneh and I. Fofana « Experimental study and analysis of corona discharge parameters on an ice surface » J. Phys. D: Appl. Phys. 37 (2004) 721–729.
- [4] C. Zener, "A Theory of the Electrical Breakdown of Solid Dielectrics", Proc. R. Soc., 145: 523-529, Lond, A July 2, 1934.
- [5] N. L. Allen and D. C. Faircloth, "Corona propagation and charge deposition on a PTFE surface", IEEE Trans. Electr. Insul., Vol. 10, No. 2, pp. 295-304, 2003.
- [6] M. Farzaneh and J. Kiernicki, "Flashover problems caused by ice build-up on Insulators", IEEE Trans. on Power Delivery, Vol. 12, No. 4, pp. 1602-1613, 1997.
- [7] I. Ndiaye, I. Fofana and M. Famaneh, « Contribution a l'étude de l'apparition et du développement des décharges couronnées a la surface de glace », CCECE 2003 – CCGEI 2003, Montréal, May/mai 2003.
- [8] I. Fofana and M. Farzaneh, "A simplified model of corona discharge development on an ice surface", IEEE Conf. Electr. Insul. Dielectr. Phenomena (CEIDP), pp. 667-670, 2004.
- [9] B. Allili, B. Zegnini, "Simulation d'un modèle physique de configuration tige-plan pour l'étude du champ d'apparition des streamers positifs sur une surface de glace", Revue des sciences et sciences de l'ingénieur, Volume 1 Numéro 1- Juin 2010 - ISSN 2170-0737, UATL, pp 67-73